PNNL-36666

Characterize and control the multi-range structure of solution-phase systems with resonant x-ray scattering

September 2024

Elisa Biasin (PI)
John L Fulton (Mentor)
Amity Andersen
Abdullah Kahraman
Mohammadhasan Dinpajooh
Shawn M Kathmann
Niri Govind
Mrinal K Bera

Prepared for the U.S. Department of Energy
under Contract DE-AC05-76RL01830

PACIFIC NORTHWEST NATIONAL LABORATORY
operated by
BATTELLE
for the
UNITED STATES DEPARTMENT OF ENERGY
under Contract DE-AC05-76RL01830

Printed in the United States of America

Available to DOE and DOE contractors from
the Office of Scientific and Technical Information,
P.O. Box 62, Oak Ridge, TN 37831-0062
www.osti.gov
ph: (865) 576-8401
fox: (865) 576-5728
email: reports@osti.gov

Available to the public from the National Technical Information Service
5301 Shawnee Rd., Alexandria, VA 22312
ph: (800) 553-NTIS (6847)
or (703) 605-6000
email: info@ntis.gov
Online ordering: http://www.ntis.gov

PNNL-36666

Characterize and control the multi-range structure of solution-phase systems with resonant x-ray scattering

September 2024

Elisa Biasin (PI)
John L Fulton (Mentor)
Amity Andersen
Abdullah Kahraman
Mohammadhasan Dinpajooh
Shawn M Kathmann
Niri Govind
Mrinal K Bera

Prepared for
the U.S. Department of Energy
under Contract DE-AC05-76RL01830

Pacific Northwest National Laboratory
Richland, Washington 99354

Abstract

This work aims at demonstrating the feasibility and impact of Anomalous X-ray Scattering (AXS) in characterizing the multi-range structures of solution-state systems. We will show preliminary investigation of long-range correlations in concentrated aqueous electrolytes with a combination of AXS and molecular dynamics (MD) simulations. We will also start exploring the capability of AXS to capture intra- and inter-molecular structure of dilute molecular systems, and specifically its sensitivity to the chemical environment surrounding active metal sites. We anticipate that the development of this method will help us to understand ion solvation and transport, which affect the performances of, for instance, electrocatalytic cells, as well as to identify/control the intrinsic structural factors that lead to selectivity, efficiency, and stability control during catalysis.

Summary

Anomalous X-ray Scattering (AXS) utilizes the energy dependence of the complex form of the atomic form factor to add chemical sensitivity to elastic x-ray scattering measurements. This method can disentangle contributions from different atom pairs, enabling a deeper understanding of short- and long-range structures in solution-phase systems.

We have conducted AXS experiments at the NSF's ChemMatCARS beamline of the Advanced Photon Source, focusing on the structural analysis of solutions. Custom liquid cells were prepared to accommodate concentrated samples, allowing sufficient X-ray transmission. The experiments utilized forward scattering geometry, capturing small- and wide-angle x-ray scattering data. Data analysis involved a Python-based software suite for automated processing, which we are currently improving – in collaborating with beamline scientist Mrinal Bera - to address challenges like fluorescence background subtraction.

Preliminary results will compare small-angle AXS signals from $ErBr_3$ aqueous solutions with all-atom MD simulations, aiming for future refinement. We will also show initial theoretical work on a bimetallic Ru-Os complex, whose electronic structure strongly depends on the solvent environment, aiming for a future AXS investigation on this system.

Acknowledgments

This research was supported by the Open Call Initiative, under the Laboratory Directed Research and Development (LDRD) Program at Pacific Northwest National Laboratory (PNNL). The project benefitted from computational resources provided by PNNL's Institutional Computing (PIC) Program. PNNL is operated by Battelle Memorial Institute for the United States Department of Energy under DOE Contract No. DE-AC05-76RL1830. NSF's ChemMatCARS, Sector 15 at the Advanced Photon Source (APS), Argonne National Laboratory (ANL) is supported by the Divisions of Chemistry (CHE) and Materials Research (DMR), National Science Foundation, under grant number NSF/CHE-2335833. This research used resources of the Advanced Photon Source, a U.S. Department of Energy (DOE) Office of Science user facility operated for the DOE Office of Science by Argonne National Laboratory under Contract No. DE-AC02-06CH11357.

Acronyms and Abbreviations

AXS	Anomalous X-ray Scattering
APS	Advanced Photon Source
MD	Molecular Dynamics
XFEL	X-ray Free Electron Laser
IP	Interaction Point
DN	Donor Number
ASAXS	Anomalous Small-Angle X-ray Scattering
AWAXS	Anomalous Wide-Angle X-ray Scattering
QM/MM	Quantum Mechanics/Molecular Mechanics
PNNL	Pacific Northwest National Laboratory

Contents

Figures

1.0 Introduction

X-ray scattering is the method of choice to probe the structure of materials, because of the direct structural relationship between the measured x-ray scattering signal and the collective set of atom positions. However, conventional x-ray scattering studies are inherently limited by their lack of element/chemical specificity. Moreover, x-ray scattering directly probes all the atomic pair distances of a sample and disentangling the different atom-pair contributions to the total scattering can be a challenging and uncertain task. Obtaining structural information of diluted molecular systems is particularly difficult since the total scattering is dominated by the solvent-solvent atom pair contribution. New approaches are needed to probe, understand, and tailor the equilibrium and non-equilibrium structure and composition of solution-phase systems, including solvated molecules and electrolytes.

Anomalous x-ray scattering (AXS) is a powerful tool to investigate local structures around a specific element (Waseda, Yoshio 2002; Bazin, Guczi, and Lynch 2002). AXS makes use of the energy dependence of the real part of the anomalous dispersion term, f ′, in the atomic form factor (see Fig. 1). When the incident x-ray energy approaches the absorption edge of a target element, the f ′ term of that element is strongly suppressed. Thus, one can extract local structural information around a selected element by using a contrast of the two scattering patterns obtained at the energies very close to and far from the absorption edge. By tuning the x-ray energy to the edges of different atom types in the sample, the different atom pair contributions to the scattering signal can be disentangled. AXS has been extensively exploited in crystallography (Hendrickson 1991). Since the method relies on relatively small differences in x-ray scattering, it requires very accurate measurements, and the application to solution-phase systems has been somewhat limited (Ludwig, Warburton, and Fontaine 1987), while no AXS studies of diluted molecular systems have been reported to date.

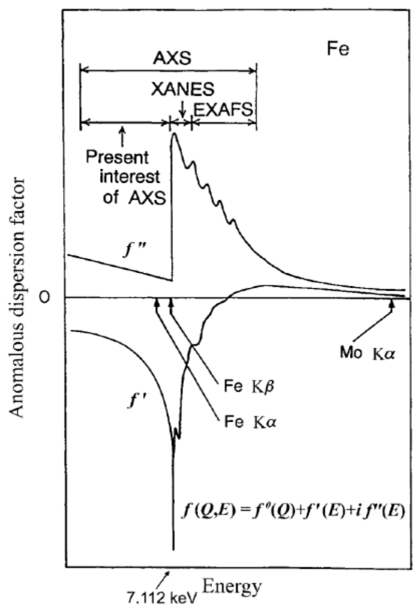

Figure 1. Energy variation of anomalous dispersion factors for Fe. From (Waseda, Yoshio 2002).

With this project we aim at developing and utilizing AXS at X-ray light sources to uniquely obtain the full set of partial structure functions for the individual pairs of chemical constituents in relevant solution-phase systems. This will allow us to go beyond the one-dimensional information available with traditional x-ray scattering and thus better understand the structure–property relationships of disordered systems, including the compositional short- and long-range order. Contrary to conventional x-ray absorption fine structure methods, both short- and long-range structural information can be derived from the AXS measurements, which is necessary to comprehensively characterize the structures of a solvated molecule and of the surrounding environments.

Specifically, we have utilized AXS to investigate the long-range ion correlations in concentrated aqueous electrolytes, as described in Section 3. Secondly, we are exploring the structural sensitivity of AXS to the chemical environment surrounding 5d-metal active catalytic sites (Section 4).

The expertise developed by this project will yield new design principle for the next generation of catalysis and their complex environment, which is important to solve the energy challenge. They will also pave the way for the implementation of AXS for *in operando* and time-resolved studies at storage ring and x-ray free electron lasers (XFELs), which are undergoing major upgrades to increase photon flux. The Linac Coherent Light Sources XFEL will deliver 1 million brilliant and ultra-short pulses per second in the hard x-ray regime by 2027. This revolutionary ability holds the promise for the successful use of time-resolved AXS to track, with unprecedented structural sensitivity, light-induced catalytic processes with femtosecond and sub-angstrom resolution.

2.0 Experimental methods

2.1 Experimental setup

The AXS experiments were performed at the NSF' ChemMatCARS (15-ID-D) beamline of the Advanced Photon Source (APS), a user facility located at the Argonne National Laboratory (Lemont, IL) in 2 different visits. The work involved close collaboration with beamline scientist Mrinal Bera. Samples were prepared onsite by diluting calculated amount of powder into solvents yielding solutions of the desired salt concentration. To allow for enough beam to transmit through the sample even for the more concentrated solution (i.e. 3 m $ErBr_3$), we couldn't use the 1.5 mm quartz capillaries normally used at the beamline and instead prepared our own liquid cells with thickness from around 100 to 500 μm. 6 inches by 6 inches peek foils from McMaster were cut into 2.5cm x 1.5cm pieces with an internal aperture of 0.5cm x 1.5cm and a 500 μm slot on top (Fig. 2a). 1 mil Kapton foil was glued on both side of the peek pieces, paying attention not to close to top slot from which the solutions were inserted into the sample holder by utilizing a thin tube connected to a syringe. The liquid cells were then mounted to an aluminum plate with 1 mm diameters holes, which was mounted at the interaction point (IP) at the beamline (Fig. 2b).

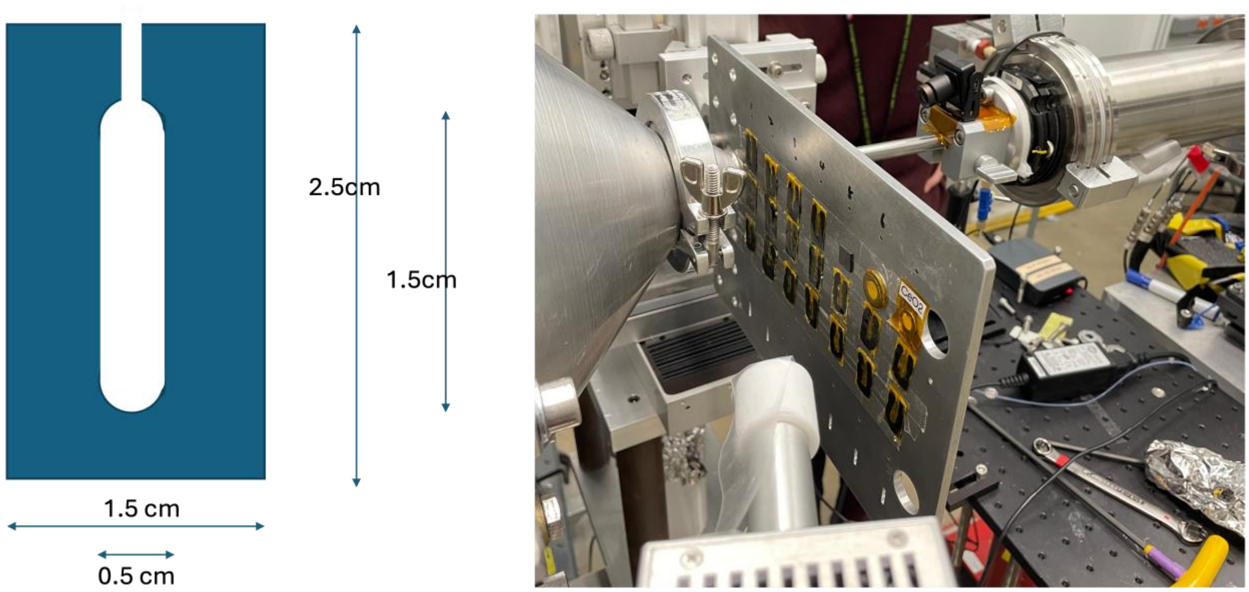

Figure 2. Experimental setup. (left) Design of the sample holder. (right) Picture of the sample plate mounted at the interaction point at beamline 15-ID-D of the APS.

We conducted the experiment in a forward scattering geometry with 2 different sample detector distances for either small- or wide-angle x-ray scattering data to be collected. The momentum transfer (Q range) for the former varied from ca. 0.05 $Å^{-1}$ to ca. 1.5 $Å^{-1}$ and the latter from ca. 0.2 $Å^{-1}$ to ca. 6 $Å^{-1}$, depending on the incident energy used. For the small-angle x-ray scattering (SAXS) configuration a vacuum tube was inserted between the IP and the detector to avoid beam loss through the air path and air scattering signal into the detector. Data frames were collected with 20 s exposure time using a Pilatus3 X 300K detector with 1mm Si chip and calibration was achieved by measuring the scattering pattern of Silver Behenate. 20 incident energies were scanned around the X-ray absorption edge of interest from around 500 eV below the edge to 20 eV above the edge by utilizing a Si(111) monochromator. A Vortex®-60EX silicon drift X-ray Fluorescence detector was utilized for energy calibration (i.e. the x-ray absorption spectrum of each sample was collected before setting up the AXS measurements) and the fluorescence signal was also collected simultaneously with the x-ray scattering signal. The scattering patterns were also collected from water for background subtraction and Glassy Carbon for absolute scale normalization at the same energies as the samples.

2.2 Data analysis

A python-based full suite of software packages with GUIs is available for automated data collection, reduction, and analysis of anomalous SAXS (ASAXS) data. Briefly the scattering images are masked for bad pixels or shaded spot in the detector, corrected for polarization, normalized by x-ray transmission, and azimuthally averaged yielding scattering signals as a function of momentum transfer Q. To eliminate scattering contribution from air and from the Kapton window (which as a Bragg peak at around 0.4 $Å^{-1}$), the signal measured for an empty liquid cell is subtracted from the samples' signals. Additionally, an energy-dependent fluorescence background needs to be subtracted from the 1D-curves. This is usually done by subtracting a flat background after identifying a Q region where the signal is unaffected by anomalous effects. Unfortunately, this is not the case for liquid samples. Our MD simulations show that the anomalous effects affect the signal in the full Q range, but slightly less in the low-Q region. For the SAXS data, we have therefore decided to offset the data according to the signal collected at around 0.2 $Å^{-1}$. More serious complications arise for anomalous wide-angle x-ray scattering (AWAXS) data. Since the fluorescence background is isotropic as a function of Q, we noticed that applying the polarization correction to an image not corrected for fluorescence contribution would lead to signal distortion and the introduction of spurious anisotropic effects. This is less of a problem for SAXS data given the smaller polarization correction needed in that region. We are now working with beamline scientist Mrinal Bera to modify the data analysis routine for WAXS so that the fluorescence background can be subtracted before the standard reduction procedure of the 2D scattering images. We are currently testing two approaches to quantify the amount of background to be subtracted:

1) Utilizing the fluorescence signal collected simultaneously to the AXS measurement. The challenge here is to find the correct scaling between the signals recorded by the two different detectors. The procedure that seems more promising assumes that fluorescence dominates the signal at the peak of the XANES spectrum.

2) Estimating the amount of fluorescence by the stoichiometry of the sample.

Because this is still work in progress, we will only show SAXS results in the remaining of the manuscript.

2.3 Data Interpretation

AXS signals can be interpreted through comparison with all atom MD simulations carried out either in a classical or QM/MM framework. Specifically, we will utilize the formalism described by Dohn *et al*. (Dohn et al. 2015) to convert radial distribution functions obtained from the MD simulations to scattering signals that can be directly compared to the data. In this formulation, the anomalous effect can be introduced by utilizing the complex form of the atomic form factor. For the preliminary data analysis shown in this report, we have utilized tabulated atomic value for the f' and f'' coefficients, but for the future we plan to obtain them from the x-ray absorption spectra utilizing the Kramers–Kronig transform.

3.0 Electrolyte solutions

3.1 Motivation

The interaction of anions with cations in aqueous solutions underlies broad areas of chemistry, electrochemistry, biochemistry, and geochemistry. To this day, there is an incomplete understanding of the interaction of simple salts such as Er^{3+} or of Sr^{2+} with Br^{-} dissolved in water. The electrostatic attractive interactions between the cation and anion are modulated by a delicate balance of different aqueous hydration effects that are not yet fully understood.

Electrostatic forces order ions from short (<1 nm) to long (1-5 nm) distances. The size domain up to 5 nm reaches the length scales (i) that can be quantitatively related to important thermodynamic properties such as ion activity coefficients and osmotic coefficients, (ii) that are important to the formation of pre-nucleation clusters at near-saturation conditions and (iii) to long range ion ordering affecting mesoscale processes. An important example is the effect of long-range Na+ ion association on the folding of DNA (Savelyev and MacKerell 2014). The long-range ordering of ionic solutions is uniquely accessible by x-ray scattering measurements. Previous x-ray scattering measurements of electrolytes aqueous solutions show the appearance of a 'prepeak' at low momentum transfer (Q<1.5 Å-1) with characteristic position and intensity depending on the type and charge of the ionic species, and on the concentration (Fetisov et al. 2020). Via comparison with MD simulations, this 'pre-peak' yields information about intermolecular structure arising from the long-range arrangements of ionic species. However, conventional x-ray diffraction studies are inherently limited by their lack of chemical specificity. In a binary MXn aqueous solution, six partial structure factors (M-O, X-O, M-M, X-X, M-X, O-O) make significant contributions to the x-ray scattering and separating the individual contributions is a difficult and uncertain task. On the contrary, all individual scattering contributions can be simply and exactly calculated from a MD trajectory. MD simulations by the CPIMS theory group at PNNL have shown that the cation−cation interaction contributes the most to the prepeak signal, which can also be reflected in the oxygen-oxygen correlations, while cation−anion and anion−oxygen pairs contribute destructively (anticorrelation) to the prepeak (Fetisov et al. 2020). Benchmarking these calculations is currently impeded by the impossibility of disentangling the different atomic pair contribution to the measured scattering signal.

In this work, we have conducted AXS of electrolytes solutions at the x-ray absorption edges of the M and X element separately to 1) disentangle the atomic pair contributions and offer unique new insights into the structure of aqueous electrolytes; 2) provide a new way to benchmark theoretical models. Our plan was to systematically study the structure of aqueous electrolytes solutions with AXS measurements as a function of changing the cations' charge and size, the anion size, and the concentration, going from very dilute conditions with no long-range ion correlation to more concentrated solutions where long-range correlations arise. By combining experiments and calculations, this study will provide a comprehensive method to link the macroscopic properties of salt solutions to the full ion-ion and ion-water pair distribution functions, thus providing unique insights on important chemical phenomena, such as ion transport and reactivity, and nucleation.

3.2 Results

We have collected ASAXS data for $ErBr_3$ (pH=1.5), $SrBr_2$, and RbBr aqueous solutions at different concentrations (from 0.25 m to 3 m). The Er and Sr data show good S/N, while the Rb data suffer from a lower scattering power of the cation (not shown). For each sample, data were collected at both the cation x-ray absorption edge (Er L-edge ~8 keV, Rb K-edge ~ 15 keV, Sr K-edge ~ 16 keV) and at the anion edge (Br K-edge ~ 13 keV). Data are interpreted though comparison with scattering signals calculated from MD simulations as described in Section 2.3.

Figure 3 shows results for 1 m $ErBr_3$ at the Er L-edge. MD simulations predicted that the amplitude of the pre-peak should decrease as a function of increasing x-ray energy approaching the Er edge. Specifically, panel b) shows contribution to the change in amplitude from the relevant atom pairs (i.e. for instance we disregard Er-H contribution given the smaller scattering power of the H atom). The decrease in intensity of the 'pre-peak' is mostly due to the Er-Er pair correlation, whose amplitude decreases 30% at the edge with respect to the pre-edge measurements. Panel c) show the measured experimental data, which indeed reproduce the trend predicted by the MD simulations and show a decrease of the 'pre-peak' amplitude as a function of increasing energy.

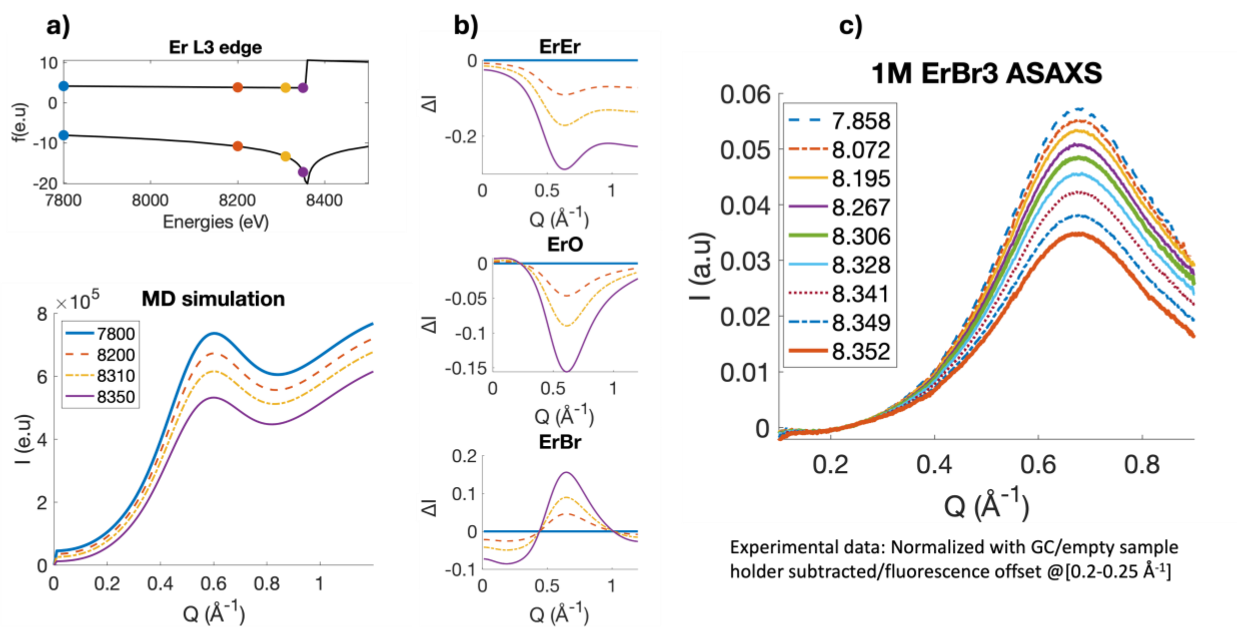

Figure 3. ErBr3 data and MD @Er edge. a) ASAXS scattering signal calculated from Molecular Dynamics simulations as a function of incident energy. b) Difference scattering signal for specific atom-atom pairs, calculated after normalizing to 1 the 'pre-peak' signal corresponding to the x-ray energy further away from the x-ray absorption maximum. c) Experimental ASAXS data as a function of energy, which reproduce the trend from MD simulations.

Figure 4 shows results for 1 m $ErBr_3$ at the Br-edge. MD simulations don't predict significant changes in amplitude, shape, or position of the 'pre-peak' as a function of incident x-ray energy. As shown in panel b), this is because the changes expected from the Br-Br contribution to the scattering signal are opposite in sign with respect to changes due to Er-Br and Br-O. Therefore, the different atom pair contributions cancel each other out. As shown in panel c), also the measured ASAXS signal don't show significant changes as a function of energy, except for a slight shift of the 'pre-peak' position to higher Q with increasing x-ray energy. This shift is more evident by taking the difference between the curves, as shown in the bottom right panel of the figure. We are currently debating the origin of such shift, which is observed also for the $SrBr_2$ sample at the Br-edge (not shown). We have currently two hypotheses:

1) If the Br-Br contribution would have an intensity maximum located at a different Q than the Er-Br and Br-O contribution, the total change due to energy scanning could potentially look like a 'pre-peak' shift. We are exploring if a change in force fields parameters could lead to such result.

2) Heating effects (which would be energy dependent) could potentially distort the solvation shell of the anion.

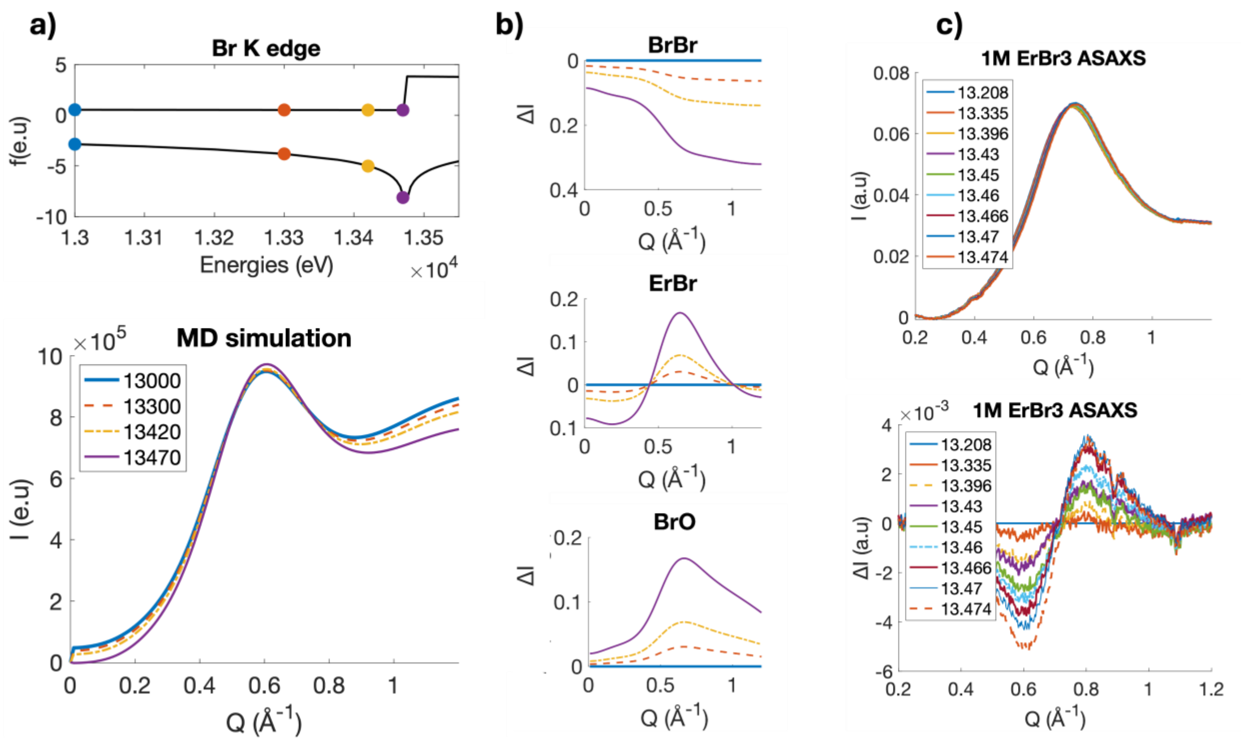

Figure 4. ErBr3 data and MD @Br edge. a) ASAXS scattering signal calculated from Molecular Dynamics simulations as a function of incident energy. b) Difference scattering signal for specific atom-atom pairs, calculated after normalizing to 1 the 'pre-peak' signal corresponding to the x-ray energy further away from the x-ray absorption maximum. c) Experimental ASAXS data as a function of energy, which show a tiny shift in the position of the 'pre-peak' as a function of energy, which is not reproduced by the simulations.

We plan to finalize the analysis of the ASAXS data as a function of cation valence and concentration, gaining new information about ion-ion and ion-water correlations in electrolyte solutions. This finding will also be combined with those obtained from the analysis of the AWAXS data, which will provide additional information on short-range interactions and ion pairing. Overall, this study will establish AXS as a new capability to probe the microscopic structure of ionic solutions beyond one-dimensional information, and to benchmark theoretical calculations.

4.0 Catalytic systems

4.1 Motivation

The efficient and selective transformation of methane, CO_2, and other small molecules into value-added chemicals remains a significant and persistent challenge. Advances require molecular-level understanding and control of the microenvironment around catalytic sites to direct reactions for key bond-making and bond-breaking steps. There is evidence that the molecular structure of the catalysts and its interactions with the surrounding solvent molecules and/or reactants, electrolytes, and other components deeply affect the chemical reaction pathway, but the mechanistic details are often unclear. This knowledge gap impedes the design of more efficient, durable, and selective catalysts.

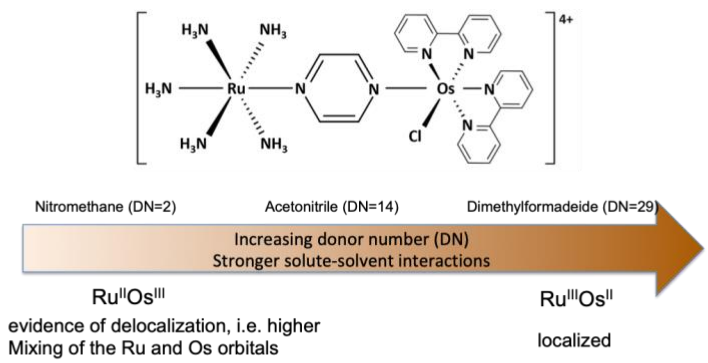

Figure 5. RuOs is a prototypical photosensitizer-catalyst unit, whose electronic structure depends on the solvent environment.

In this project we plan to explore the structural sensitivity of AXS to the intra- and inter-molecular structure of solvated catalysts. We will initially focus our studies on investigating bi-metallic catalysts containing 5d transition metals (Ir, Re, Pt, Os), since the anomalous effect at the real part of the anomalous dispersion term has substantially larger value (over 30%) at the L-shell absorption edge. For 5d elements, the L-edge lie in the energy range available at synchrotron light sources (~9-13 keV). As representative of these systems, we have started theoretical investigation of a Ru-Os complex, whose structure in shown in Fig. 5.

Ru-Os is reported to be Ru^{III}-Os^{II} in high donor number solvents (i.e. solvents that can form strong hydrogen bond interactions) and Ru^{II}-Os^{III} in low donor number solvents (Hupp, Neyhart, and Meyer 1986). The implied difference in electronic structure lies in H-bonding interactions between the NH_3 ligand of the Ru and the surrounding solvent molecules. In addition, there are spectroscopic evidence of higher electronic delocalization between the two metals in the Os^{III}-Ru^{II} molecule with respect to Os^{II}-Ru^{III}. The molecular mechanisms that lead to this observed behavior are to be understood and in this project we aim at utilizing AXS to detect difference in intra- and inter- molecular structure in Ru^{II}-Os^{III} and Ru^{III}-Os^{II} by measuring the complex in two different environments, specifically nitromethane (NTM, DN =2) and dimethylformamide (DMF, DN=24).

A charge transfer reaction can also be photoinduced by exciting in the near-IR (metal-to-metal charge transfer band). Therefore Ru-Os is also an ideal candidate for time-resolved AXS studies, – when the capability will become available, as describe in the Introduction – which will allow us to probe intramolecular excited state dynamics and the coupled solvation reorganization with exquisite sensitivity (Biasin et al. 2021).

4.2 Results

We have started a theoretical investigation by carrying out MD simulations that will allow us to predict the expected anomalous scattering signal at the Os L-edge and Ru K-edge. Specifically, we are utilizing a quantum mechanics/molecular mechanics (QM/MM) framework, where the RuOs molecule was treated at the QM level and the surrounding solvent at the classical level. This framework has allowed us to reproduce the different electronic structure in the different solvent environments, as described in detail below.

The atomistic structure model of the RuOs complex was built with the Materials Studio software as well as the atomistic structure models of the dimethylformamide and nitromethane molecules. The PACKMOL software was used to create two small boxes of dimethylformamide solvent and nitromethane solvent to optimize then equilibrate with classical MD using the NWChem computational chemistry suite (Aprà et al. 2020). The dimethylformamide and nitromethane boxes had target densities of 0.944 g/cm^3 and 1.14 g/cm^3, respectively. The equilibrated boxes were used as solvent templates to solvate the RuOs complex in large 60^3 Å^3 boxes. To neutralize the the 4+ charge of the RuOs complex, four chloride ions were placed in the box. Appropriate force fields were utilized for all atoms.

Following the setup of the two initial large boxes of dimethylformamide-solvated RuOs complex and nitromethane-solvated RuOs complex, these two systems were optimized with at most five cycles of BFGS optimization of the RuOs complex (QM region) followed by conjugate gradient optimization of the solvent region with the QM RuOs complex region held fixed and represented with ESP fitted charges. For the QM region (the RuOs complex), the 6-311G** basis set was used for all light atoms (H, C, and N). For the heavier Ru, Os, and Cl atoms the Stuttgart effective core potentials and basis sets were used in the RuOs complex. The PBE0 hybrid density functional was used for the QM region for all QM/MM simulations. Following optimization of each of the two RuOs complex-solvent systems, the two systems were equilibrated with Berendsen thermostat NVT molecular dynamics (temperature set at 298.15 K) for 500 ps with the complex held fixed and represented with ESP fitted charges from an initial quantum chemistry calculation. SHAKE constraints were used to fix the bond lengths of the hydrogen bearing bonds in the dimethylformamide and nitromethane molecules. With these constraints the time step could be set at 2.0 fs. Following this initial equilibration of these two systems, the constraint on the complex was removed, and the solvated complex systems were equilibrated for another 2.5 ps with the complex updating with a QM calculation on the complex every time step. For these QM/MM MD simulations, the time-step was reduced to 0.25 fs. Equilibration was deemed achieved when each of the solvated complex systems showed the expected spin charge for the Ru and Os atoms (Fig. 7 top). For this, the Mulliken spin charge was monitored throughout these MD simulations. Once the correct spin charges were achieved, the QM/MM MD production runs were performed for 10 ps.

Radial distribution functions were calculated from the final production runs. Representative RDFs are shown in Fig. 7. Intramolecular structural changes are present between Ru^{II}-Os^{III} (in DMF) and Ru^{III}-Os^{II} (in NMT). Specifically, the bond length between Os and Ru is slightly shorter (0.04 Å) in NMT, in agreement with a more delocalized electronic structure. Surprisingly, the Os-Cl bond is ca. 0.1 Å shorter in NMT with respect to in DMF. This is consistent with the fact that there is some spin density shared between the Os and Cl in NMT. Finally, as expected, a more-structured solvation shell surrounds the Ru part of the molecule in DMF, in agreement with the fact that there should be H-bonding between the Ru NH_3 ligands and the DMF molecules. We hope that these predicted structural changes can be confirmed with AWAXS soon. To calculate the expected anomalous effects in the scattering signals, we are currently running the production run for longer, since more statistic is needed for a reliable estimation. The sample has been synthesized by the group of Eric Wiedner at PNNL and we have carried out characterization of the sample with x-ray absorption spectroscopy. A manuscript is in preparation.

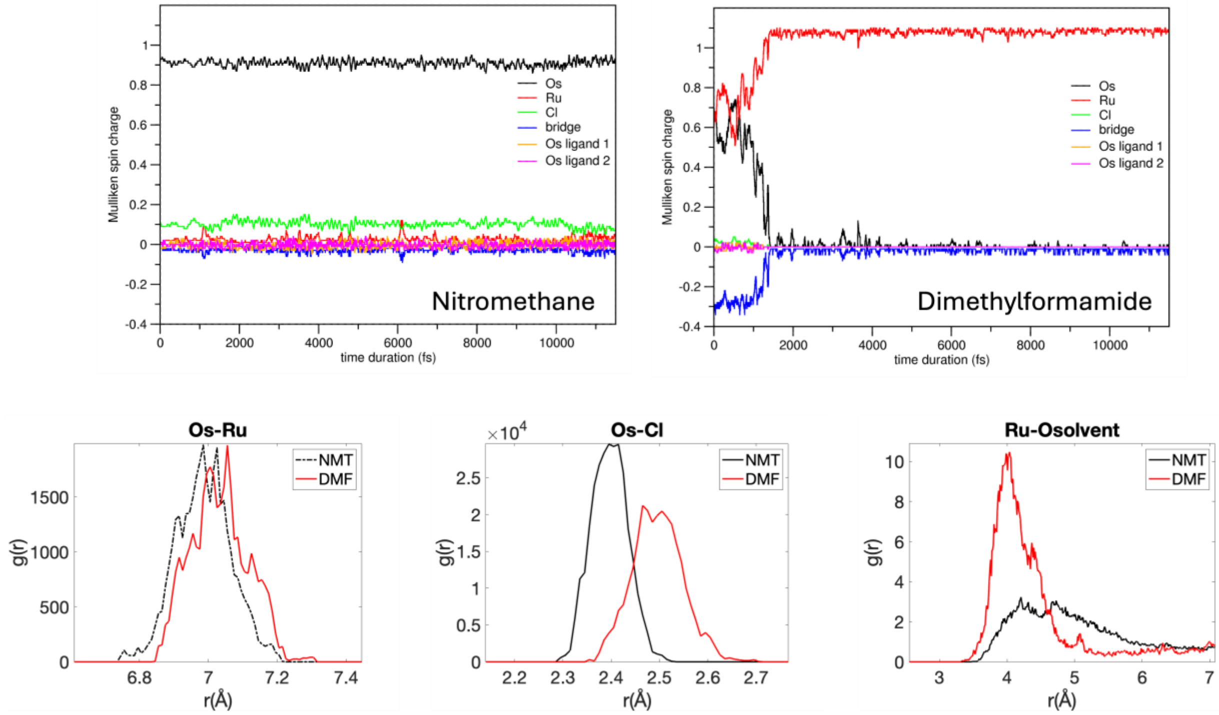

Figure 6. Figure 7. Results of RuOs QM/MM MD simulations. (top) Mulliken spin charge as a function of simulation time for chemical components of the nitromethane-solvated RuOs complex (left) and of the dimethylformamide-solvated RuOs complex (right). (bottom) Comparison of representative RDFs of the RuOs system in the two different solvent environments.

5.0 References

Aprà, E., E. J. Bylaska, W. A. de Jong, N. Govind, K. Kowalski, T. P. Straatsma, M. Valiev, et al. 2020. "NWChem: Past, Present, and Future." *The Journal of Chemical Physics* 152 (18): 184102. https://doi.org/10.1063/5.0004997.

Bazin, D., L. Guczi, and J. Lynch. 2002. "Anomalous Wide Angle X-Ray Scattering (AWAXS) and Heterogeneous Catalysts." *Applied Catalysis A: General* 226 (1): 87–113. https://doi.org/10.1016/S0926-860X(01)00892-4.

Biasin, Elisa, Zachary W. Fox, Amity Andersen, Kathryn Ledbetter, Kasper S. Kjær, Roberto Alonso-Mori, Julia M. Carlstad, et al. 2021. "Direct Observation of Coherent Femtosecond Solvent Reorganization Coupled to Intramolecular Electron Transfer." *Nature Chemistry* 13 (4): 343–49. https://doi.org/10.1038/s41557-020-00629-3.

Dohn, Asmus O., Elisa Biasin, Kristoffer Haldrup, Martin M. Nielsen, Niels E. Henriksen, and Klaus B. Møller. 2015. "On the Calculation of X-Ray Scattering Signals from Pairwise Radial Distribution Functions." *Journal of Physics B: Atomic, Molecular and Optical Physics* 48 (24): 244010. https://doi.org/10.1088/0953-4075/48/24/244010.

Fetisov, Evgenii O., Christopher J. Mundy, Gregory K. Schenter, Chris J. Benmore, John L. Fulton, and Shawn M. Kathmann. 2020. "Nanometer-Scale Correlations in Aqueous Salt Solutions." *The Journal of Physical Chemistry Letters* 11 (7): 2598–2604. https://doi.org/10.1021/acs.jpclett.0c00322.

Hendrickson, Wayne A. 1991. "Determination of Macromolecular Structures from Anomalous Diffraction of Synchrotron Radiation" 254 (5028): 55–58.

Hupp, Joseph T., Gregory A. Neyhart, and Thomas J. Meyer. 1986. "Solvent Control of Oxidation State Distribution and Electronic Delocalization in an Osmium-Ruthenium, Mixed-Metal Dimer." *Journal of the American Chemical Society* 108 (17): 5349–50. https://doi.org/10.1021/ja00277a052.

Ludwig, K. F., W. K. Warburton, and Alain Fontaine. 1987. "X-ray Studies of Concentrated Aqueous Solutions." *The Journal of Chemical Physics* 87 (1): 620–29. https://doi.org/10.1063/1.453556.

Savelyev, Alexey, and Alexander D. Jr. MacKerell. 2014. "Balancing the Interactions of Ions, Water, and DNA in the Drude Polarizable Force Field." *The Journal of Physical Chemistry B* 118 (24): 6742–57. https://doi.org/10.1021/jp503469s.

Waseda, Yoshio. 2002. *Anomalous X-Ray Scattering for Materials Characterization*. Springer.

Pacific Northwest National Laboratory

902 Battelle Boulevard
P.O. Box 999
Richland, WA 99354

1-888-375-PNNL (7665)

www.pnnl.gov